

Development of a Sub-100nm Integrated Imaging System Using Chromeless Phase-Shifting Imaging with Very High NA KrF Exposure and Off-axis Illumination

John S. Petersen¹, Will Conley², Bernie Roman², Lloyd Litt², Kevin Lucas², Wei Wu², Doug Van Den Broeke³, J. Fung Chen³, Tom Laidig³, Kurt Wampler³, David J. Gerold¹, Robert Socha⁴, Judith van Praagh⁵, Richard Droste⁵

¹ Petersen Advanced Lithography, Inc., 12325 Hymeadow DR, Building 2, Suite 201, Austin, TX 78750

²Motorola, Digital DNA Labs, Austin, TX 78721

³ ASML MaskTools, 4800 Great American Parkway #400, Santa Clara, CA 95054

⁴ ASML TDC, 4800 Great American Parkway #400, Santa Clara, CA 95054

⁵ ASML, 1100 DeRun, Veldhoven, Netherlands

email: jppetersen@advlitho.com

1.0 Abstract

Examining features of varying pitch imaged using phase-shifting masks shows a pitch dependence on the transmission best suited for optimum imaging. The reason for this deals with the relative magnitude of the zero and higher diffraction orders that are formed as the exposing wavelength passes through the plurality of zero and 180-degree phase-shifted regions. Subsequently, some of the diffraction orders are collected and projected to form the image of the object. Chromeless Phase-Shift Lithography (CPL) deals with using halftoning structures to manipulate these relative magnitudes of these diffraction orders to ultimately construct the desired projected image. A key feature of CPL is that with the ability to manipulate the diffraction orders, a single weak phase-shifting mask can be made to emulate any weak phase-shifting mask and therefore the optimal imaging condition of any pattern can be placed on a single mask regardless of the type of weak phase-shifter that produces that result. In addition, these structures are used to render the plurality of size, shape and pitch such that the formed images produce their respective desired size and shape with sufficient image process tolerance. These images are typically made under identical exposure conditions, but not limited to single exposure condition. These halftoning structures can be used exterior, as assist features, or interior to the primary feature. These structures can range in transmission from 0% to 100% and they can be phase-shifted relative to the primary features or not. Thus CPL deals with the design, layout, and utilization of transparent and semi-transparent phase-shift masks and their use in an integrated imaging solution of exposure tool, mask and the photoresist recording media. This paper describes the method of diffraction matching, provides an example and reviews some experimental data using high numerical aperture KrF exposure.

Keywords: Chromeless PSM, CLM, high NA, off-axis illumination, OAI, OPC, PSM, halftone, mask fabrication, Integrated Imaging System

2.0 Introduction

One method for tuning the magnitude of the diffraction orders is to use weak phase shift masks. These masks work by allowing exposure radiation to pass through objects in a fashion that creates a difference in phase between coherently linked points while having an imbalance in the electric field between the shifted regions due to a difference in their complex transmittance. Several types of these masks are known in the art as the rim, attenuated or embedded (or incorrectly named halftone), and transparent (or chromeless) shifter-shutter (Figure 1) phase-shifting masks. They all form their phase-shift differently but they all yield a zero diffraction order of smaller amplitude with the lost energy distributed to the higher diffraction orders. Which ratio of first to zero diffraction order magnitude is optimal depends on the pitch of the feature being imaged along with the shape of the illuminator and the desired printing size in the developed photoresist. For the best imaging performance, these tuned diffraction patterns are then used with off-axis illumination to image smaller pitches with better tolerance to imaging process variation.

Until now, manipulation of the amplitude ratio of zero-first diffraction orders was restricted to using certain weak phase-shifting techniques with biasing and with sub-resolution assist features. In particular, for the attenuated shifter, transparency of the shifter materials was adjusted and then used along with

biasing and with the use of sub-resolution assist features (Figure 1).¹ Transparency typically ranges from 3% to 10%, with higher transmissions from 10% to 100% being reported to be optimal for pitches where the space is larger than the dark line.² This 100% transparent attenuated phase-shifting technology is the previously mentioned, chromeless shifter-shutter (Figure 2).³ In this technique, phase -edges of a pattern are placed within 0.2 to 0.3 times the exposing wavelength divided by the numerical aperture of the projection lens.⁴ For lines larger or smaller than this, the destructive interference is insufficient to prevent exposure in the area that is supposed to not be exposed. Printing features larger than this is accomplished in one of two ways. The first places an opaque layer in the region that is to stay dark with the feature edges being opaque or rim-shifted⁵ (Figure 3). The second creates a dark grating by placing a series of features whose size meets the criteria for printing an opaque line using chromeless technology (Figure 4).⁴

In the past printing smaller features is accomplished by changing the exposing wavelength and the numerical aperture of the exposure tool. The dark grating technique has susceptibility for defects incurred during the mask fabrication to print during the imaging process. In addition, chromeless phase shifting is known not to work with off-axis as the shifter and shutter sizes approached each other in size. This is because the integrated electric fields of the two opposing phase-shifted regions are equal and this balanced condition (Figure 5) cancels the zero diffraction order making it impossible to get the prerequisite zero diffraction order needed for using off-axis illumination. To summarize, each weak phase-shifting technique solved certain imaging problems but not universally so and with some severe limitations.

3.0 Summary of CPL

We first published our results in 2001.⁶ In that paper we discussed the shifter-shutter mask called CLM. We now want to discuss the way this patented technique works.⁷ Chromeless Phase-shift Lithography removes these barriers to manipulation of the amplitude ratio of the zero-first diffraction order by using halftoning of opaque and phase-shifted transparent/semitransparent structures within the primary feature (Figure 6) and as sub-resolution assist features (Figure 7). The reason for this, deals with the relative magnitude of the zero and higher diffraction orders that are formed as the exposing wavelength passes through the plurality of zero and 180-degree-shifted regions (Figure 6, 9A and 10B). Subsequently some of the diffraction orders are collected and projected to form the image of the object. CPL deals with using halftoning structures to manipulate these relative magnitudes of these diffraction orders to ultimately construct the desired projected image. At the resolution limit of the mask maker, this is especially useful for converting strong shifted, no zero diffraction order, equal line and space chromeless phase edges to weak phase shifters that have some zero order (Figure 6). Halftoning creates an imbalance in the electric field between the shifted regions that results in the introduction of zero diffraction order and makes these features compatible with the other shifter-shutter chromeless features found amongst the many types of objects used in making a semiconductor circuit. Previously, this was done by decreasing the size of the primary feature so that a shifter-shutter structure was formed, but does not work when the mask maker cannot reliably produce the desired pattern.

Examining features of varying pitch size imaged using phase-shifting masks shows a pitch dependence on the transmission best suited for obtaining the same size resist image for a given exposure condition (Figure 8). Figure 8A shows the imaging result for different combinations of attenuated phase-shift mask transmittance and space sizes between 100nm features. The figures at the intersections of each condition of transmittance and space size are PROLITH™ (KLA-Tencor) simulated cross-sections of developed photoresist images that were exposed at 22 mJ/cm² and -0.15 microns using a 0.70 NA, 248nm exposure tool with quadrupole illumination. The images surrounded by the boxes have a resist image size between 90 and 110nm. These sizes are used here to arbitrarily define the lower and upper limits for acceptable sizing. Images outside of the boxed area did not meet this criterion. The contour map in Figure 8B shows the same information. As an example of the technique, Figures 8A and 8B show that in the range of 20 to 30% transmittance that the figures meet the sizing criteria of plus minus ten percent of 100nm for this exposure condition for a 400nm pitch and that a 600nm pitch sizes with a transmittivity of 100%. These features will not image together without the use of CPL (Figure 8C). The left graph in Figure 8C shows that the exposure and focus conditions for attaining 100nm lines for 600nm and 400nm pitches are totally

separate, with no common process corridor. The graph on the right in Figure 8C shows the exposure latitude for different amounts of defocus.

In this CPL example, first, for the 400nm pitch structure, a 100% transmittance chromeless phase-shift mask will be halftoned and biased to produce a diffraction pattern that nearly matches the aerial image produced with a 26% attenuated phase-shift mask (Figure 9). Then the 600nm pitch structure will be dealt with using halftoned, chrome scattering bars and the 400nm and 600nm features will be compared (Figure 10). Starting at the top left corner and moving clockwise, Figure 9A shows for the 400nm pitch structure the non-halftoned, 26% attenuated phase-shift mask, the halftoned 100% chromeless phase-shift mask, the top down view of the halftoned mask's aerial image and finally the diffraction order map for both attenuated and halftone chromeless mask. Notice the near perfect overlay of the two diffraction patterns and that the top down aerial image of the halftoned chromeless mask shows no sign of the discrete halftoning objects. Figure 9B shows the simulated focus-exposure results of the masks described in Figure 9A. Starting clockwise from the top left corner, the plot shows the process window for allowed variations of focus and exposure to maintain the resist image size between 90nm and 110nm for the 26% attenuated phase-shift mask, the same for the halftone chromeless mask, the exposure latitude versus depth of focus for each mask, and the overlap of the process windows. To convert the 100% chromeless phase-shift mask to a 26% attenuated-like phase-shift mask required increasing the width of the 100nm line to 115nm and halftoning said line using a 180nm halftone pitch with a 67% duty cycle of 180 degree shifter to non-shifter region.

For the 600nm pitch, structure sizing the 100nm line at the same time as the 400nm pitch is attained using halftoned chrome scattering bars (Figure 10). Figure 10A shows clockwise from the top left, the 600nm pitch unmodified feature, the 400nm pitch feature, the halftone 400nm pitch layout described in Figure 9 and the 600nm pitch with chrome scattering bars. Figure 10B shows the diffraction orders for their respected pitches and modifications as outlined in Figure 10A. Figure 10C shows for the two modified masks the common focus-exposure process window that sizes the 100nm line for both the 400nm and 600nm pitch structures. Clockwise from the top left the graphs are the 600nm pitch feature layout with chrome scattering bars, halftone chromeless 400nm pitch layout, the common percent exposure latitude relative to defocus for both pitches, and the common focus-exposure process window.

These simulation examples show that a chromeless mask can be halftoned to behave as an attenuated phase-shift mask of lower transmittance. In addition, Figure 10C shows that these structures are used to render the plurality of size, shape and pitch such that the formed images produce their respective desired size and shape with sufficient image process tolerance. These images are typically made under identical exposure conditions, but not limited to single exposure condition. These halftoning structures can be used exterior, as assist features, or interior to the primary feature. These structures can range in transmission from 0% to 100% and they can be phase-shifted relative to the primary features or not. Figure 11 shows how the focus-exposure process window is enhanced using scattering bars to suppress zero diffraction order. Clockwise from the top left shows the diffraction order for an uncorrected 100nm line with a 600nm pitch, the diffraction orders for a corrected layout, the process window for the corrected layout, and the process window for the uncorrected layout. Note that the corrected mask has four times the depth of focus of the uncorrected mask.

Experimentally, Figure 12 shows through focus images of resist for pitches of 240nm, 260nm, 300nm, 350nm, 500nm, 600nm, 700nm and 1200nm targeted to size at 100nm. Exposure was made with a 248nm, ASML PAS 5500/800 0.8 NA, and quasar illumination with inner sigma of 0.57 and outer of 0.87. The top of the resist is rounded and is an artifact that is often observed with thin resist films, but it is not clear what causes it. Overall, there do not appear to be any forbidden pitches. Figure 13 shows focus-exposure linewidth results for pitches of 240nm, 260nm, 300nm, 350nm, 500nm, 600nm, 700nm and 1200nm whose cross-sections were shown in Figure 12. These results were made with a first generation CPL mask, CLM001. Even though this mask was designed using a primal diffraction-matching algorithm and coarse, 10nm incremental bias corrections, the common process window looks good. The common depth of focus for all the pitches was 0.38 μ m with 6% exposure latitude with each individual pitch having 0.50 μ m or more DoF with 10% exposure latitude. The masks and the performance are described in Table 1.

These data were gathered with a KLA 8100, low voltage SEM. Correlation to cross section shows that on average the top-down measurements are 11.4 nm larger than the cross sections but because of a strong

dependence on focus and pitch, the difference between top-down and cross-section is not constant, making simple correction inappropriate. Figure 14 shows the correlation analysis that describes this dependence. In this analysis, we varied the function of the independent variables for all the Figure 13 pitches, except for the 300nm pitch (case 152) for which there was no cross-section measurements, and then using the method of stepwise regressions isolated the strongest dependence that also gave the best correlation function, the best lack of fit and F-test results. In this regression analysis, except for focus, the regressor form was changed to get the best possible fit, pitch was examined unmodified and as its natural log, and dose was examined unmodified, as its reciprocal and as its natural log. Figure 14 shows the results of correlation, (a), correlation plot, (a'), the estimate of the parameters, (b), an interactions plot, (b'), and Pareto analysis, (c) of the best manipulation of the independent variables for 176 images made with exposures from 22 to 34 mJ · cm⁻² and -0.1, 0.0 and +0.1µm of focus. These results show that the correlation was poor at 0.57 but as the F-tests indicate, the tendencies are likely correct. Further, the lack-of-fit analysis suggests that the correct regressors may still need refinement. Nevertheless, there appears to be an interaction between pitch and focus. The Pareto ranking is focus followed by third order log(pitch), second order log(dose), first order focus-log(pitch) interaction, log(pitch) and third order log(dose). While this analysis suggests that we could use the regressions equation to adjust the data for subsequent re-analysis of the process windows, the lack of fit does not encourage us to do so especially where we would extrapolate the correction. Suffice it to say that development of 100nm and sub-100nm imaging processes need more data than can be gathered by SEM alone and that other methods like electrical linewidth and scatterometric methods should be explored to finalize refinement of an integrated imaging system.

Figure 15 shows from the imaging of a 6 transistor SRAM with a cell pitch of 1085nm in the x-orientation. The figures from left to right are: a hybrid mask, the mask's diffraction pattern convolved with the source and the final resist image. Using phase shifted assists helped weight the first diffraction order and dampen the higher orders. The images are sized at a 100nm nominal.

4.0 Summary

CPL deals with the design, layout, and utilization of transparent and semi-transparent phase-shift masks and their use in an integrated imaging solution of exposure tool, mask and the photoresist recording media. CPL removes barriers to manipulation of the amplitude ratio of the zero-first diffraction order. This is accomplished using halftoning structures to manipulate these relative magnitudes of these diffraction orders to ultimately construct the desired projected image. In addition, these structures are used to render the plurality of size; shape and pitch such that the formed images produce their respective desired size and shape with sufficient image process tolerance. These images are typically made under identical exposure conditions, but not limited to single exposure condition. These halftoning structures can be used exterior, as assist features, or interior to the primary feature. These structures can range in transmission from 0% to 100% and they can be phase-shifted relative to the primary features or not. This CPL deals with the design, layout, fabrication and utilization of transparent and semi-transparent phase-shift masks and their use in an integrated imaging solution of exposure tool, mask and the photoresist recording media.

5.0 Acknowledgements

I wish to thank all my co-authors for their effort in this work. In particular, I want to highlight the support of my good friends and colleagues J. Fung Chen (ASML MaskTools), Robert Socha (ASML), Doug VanDenBroeke (ASML MaskTools) and Will Conley (Motorola). I'll see you at 45nm. I also want to thank ASML MaskTools and ASML for the financial support during this period and for making a diligent effort to design what I believe to be the first true integrated imaging system. In addition, I would like to thank KLA-Tencor for the PROLITH™ and ProDATA™ support and the ongoing support of my research and my company.

Figure 1 shows an example of a transparent or chromeless shifter-shutter-type weak phase-shift mask.

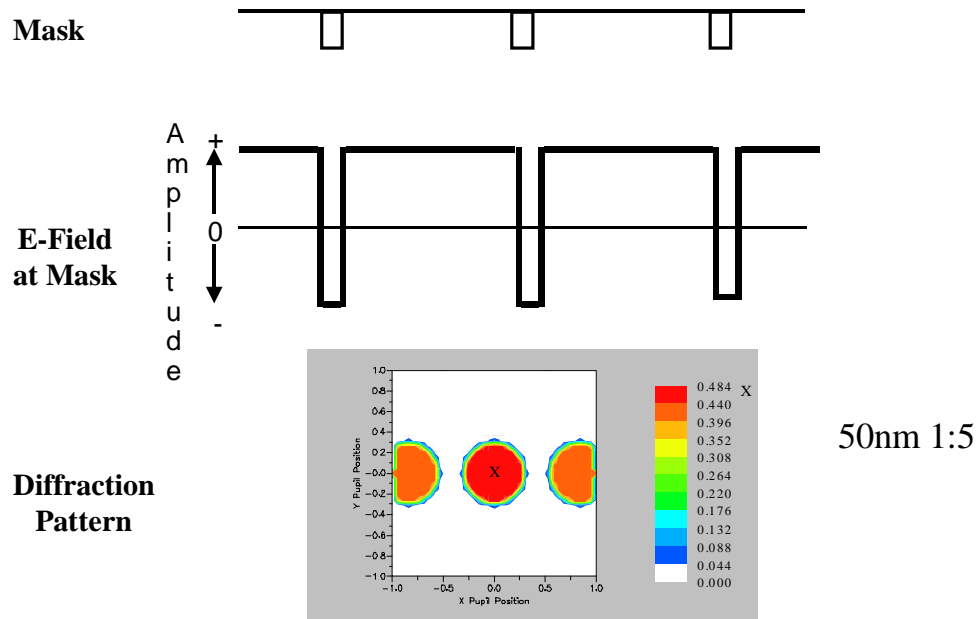


Figure 2 shows an example of a CPL mask using sub-resolution assist features.

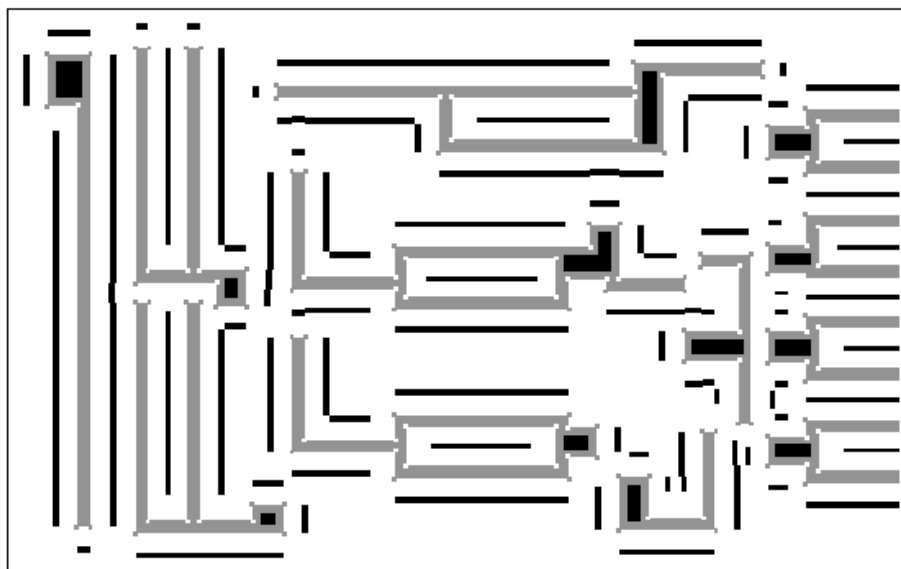


Figure 3 shows using an opaque feature to prevent imaging problems for features whose phase edges are too far apart to effectively eliminate undesired exposure. 3a shows opaque feature with no rim and 3b shows the same feature but is rim-shifted to make a darker edge.

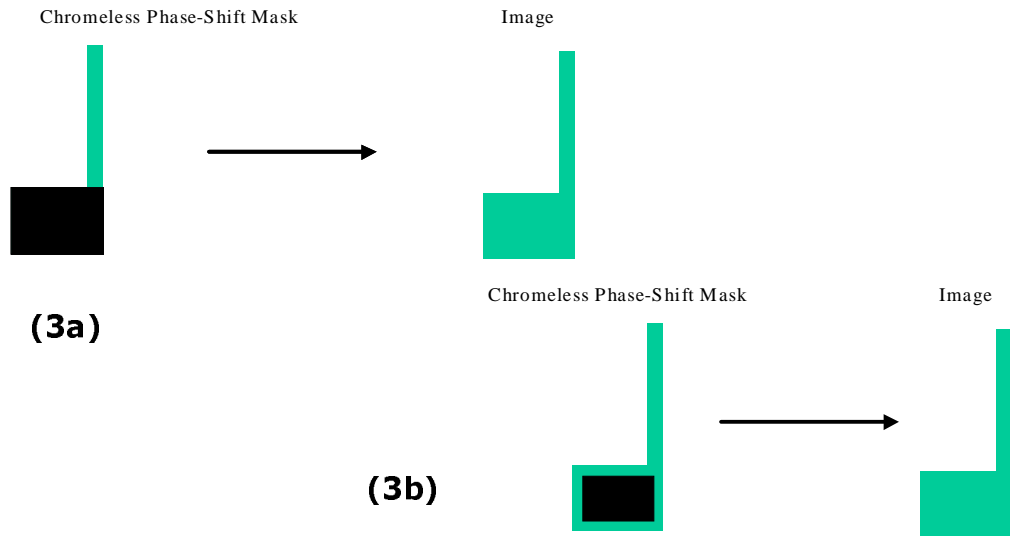


Figure 4 shows the use of a chromeless dark grating as an opaque feature to prevent imaging problems for features whose phase edges are too far apart to effectively eliminate undesired exposure.

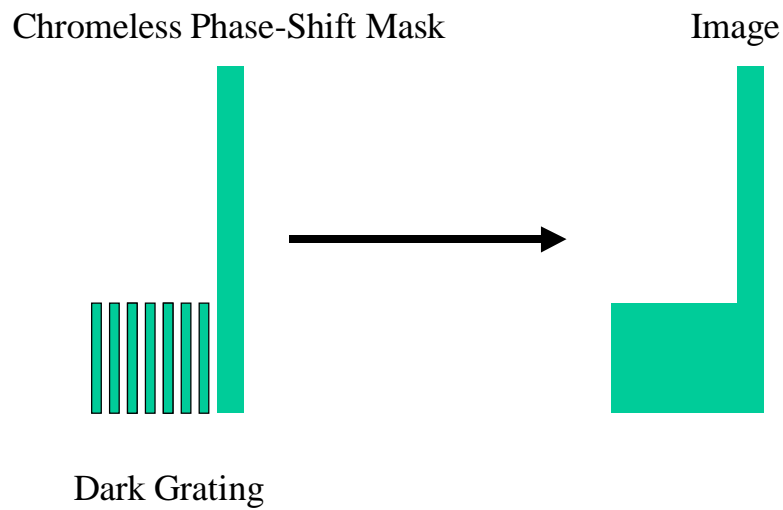


Figure 5 shows an example of a chromeless strong phase-edge mask and its electric field.

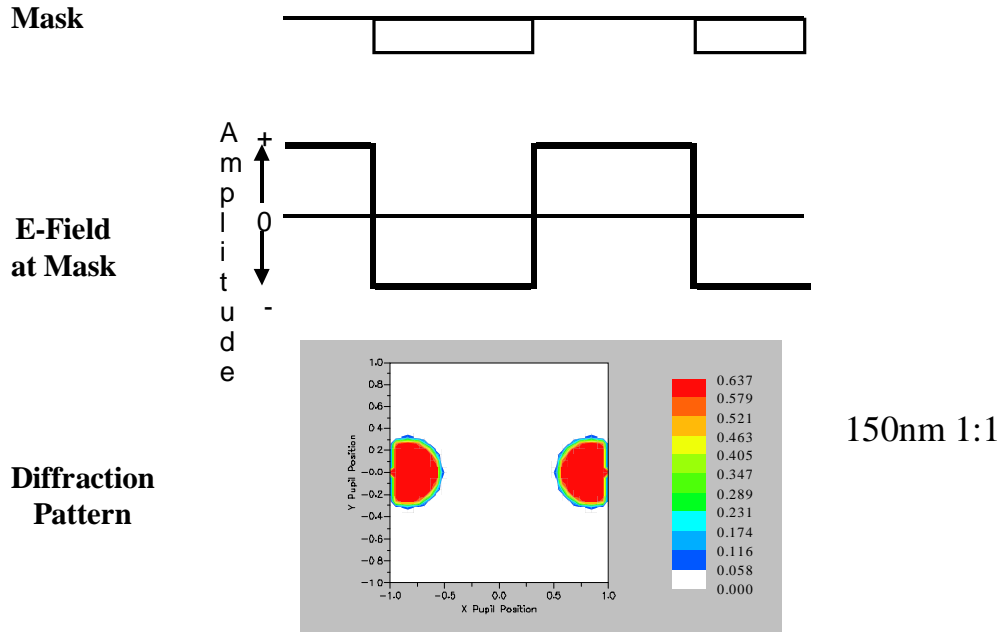


Figure 6 shows halftoning of a primary feature so that it has optimal zero-first diffraction order amplitude using a chromeless shifter-shutter phase-shifting mask. 18A shows primary features before (on the left) and after (on the right) halftoning. 18B compares the diffraction patterns of an equal line space chromeless pattern to that of the same structure halftoned. Without halftoning, there is no zero diffraction order but there is with halftoning making it possible to use off-axis illumination for these for dense features.

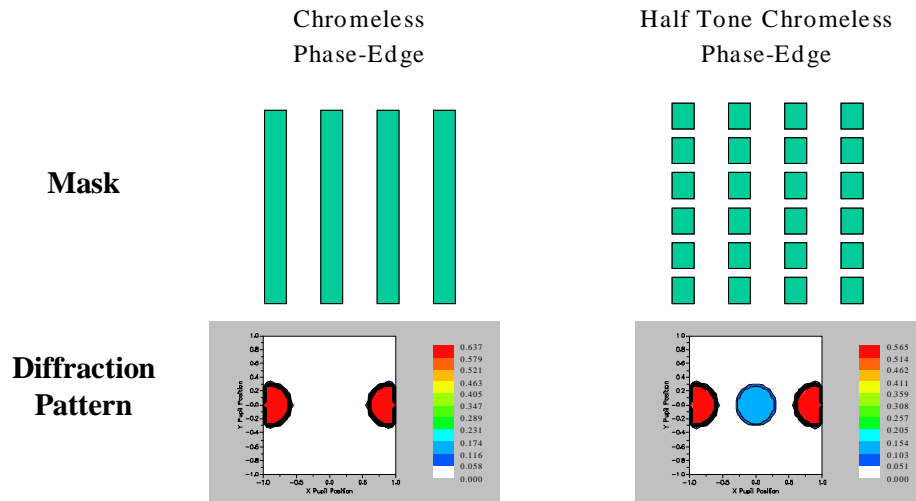


Figure 7 shows halftoning of a scattering bar assist feature so that it makes its associated primary feature have an optimal zero-first diffraction order amplitude using a chromeless shifter-shutter phase-shifting mask.

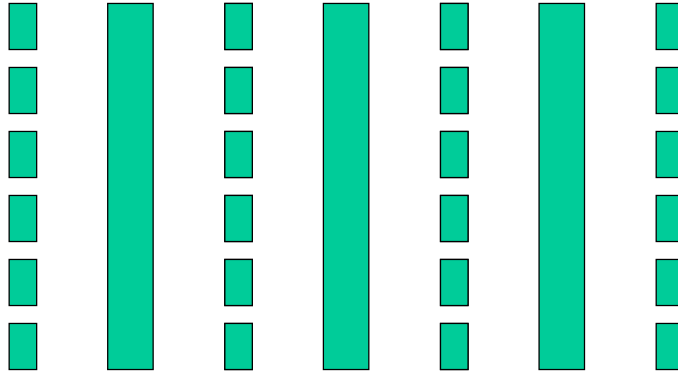
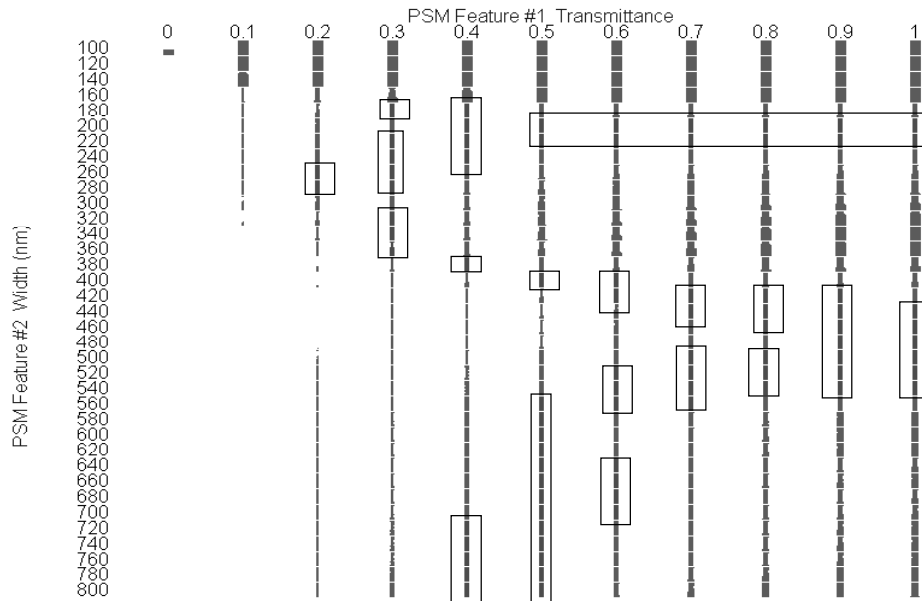


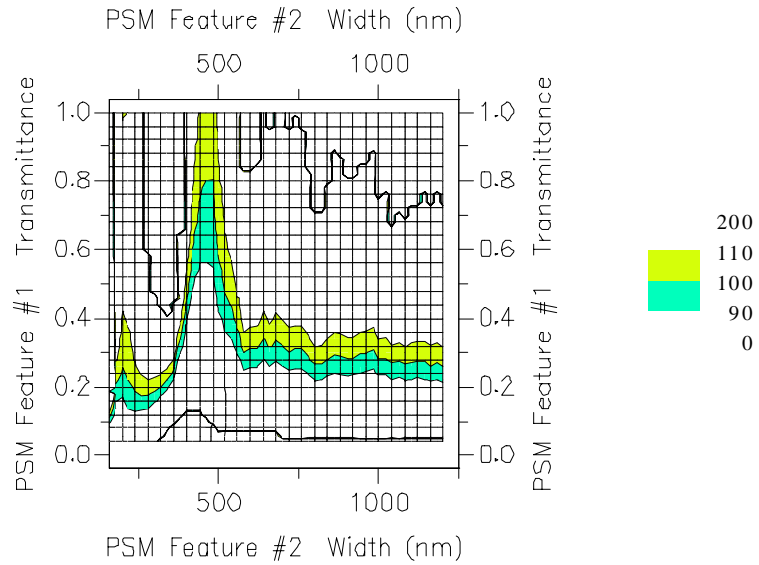
Figure 8 shows for 100nm lines and spaces ranging in size from 100nm to 800nm the transmissivity of the phase-shift required to produce a 100nm line for each pitch.

8A shows simulated resist images for each condition of pitch and transmissivity. The box outlines in the figure show resist images that meet the feature size acceptance criteria of 90nm to 110nm.



Feature size = 100nm

8B shows another graphical representation of the same data.



22mJ/-0.15 micron

Figure 8c shows that there is no focus-exposure common process window but both features have reasonable exposure latitude-DoF response.

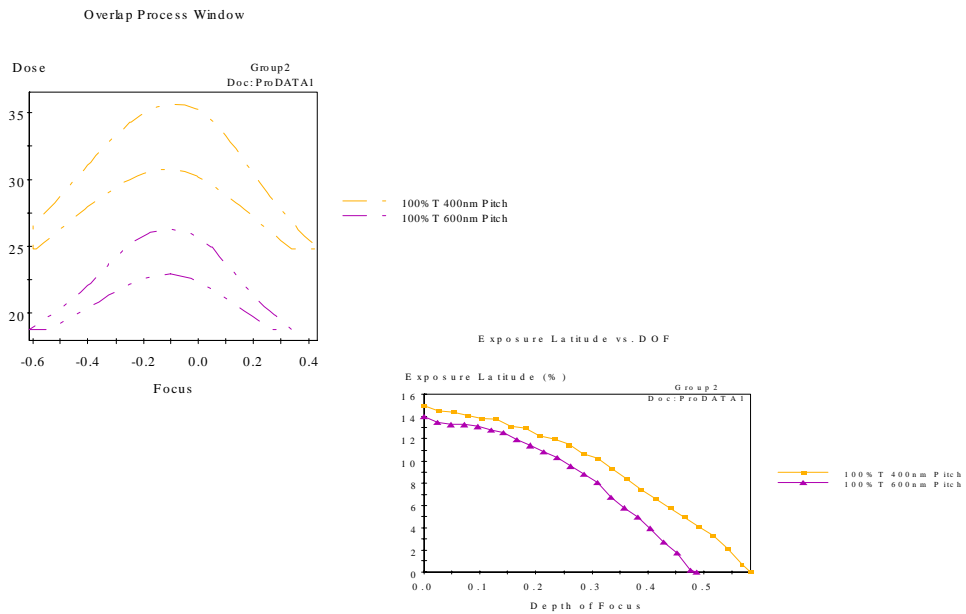
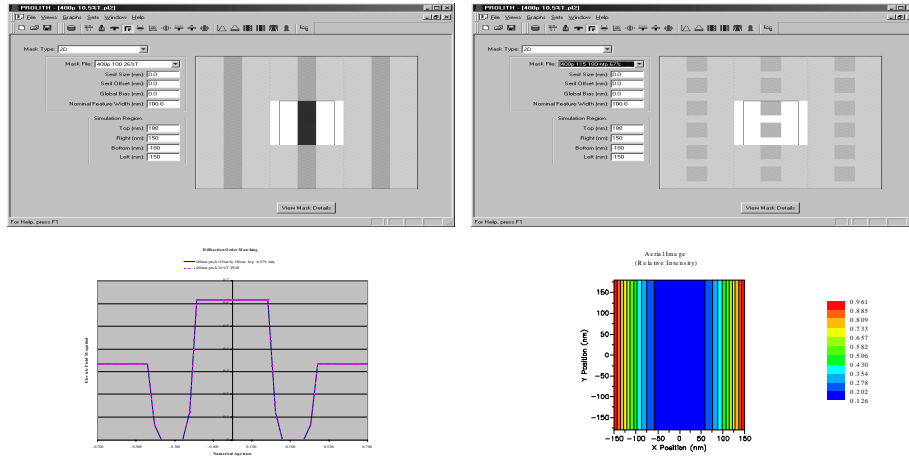


Figure 9 shows how an attenuated phase-shifting mask can be made from an unattenuated, chromeless phase-shifting mask so that, in this example, the 100nm line of a 400nm pitch structure can be imaged the same way as if it were the attenuated mask.

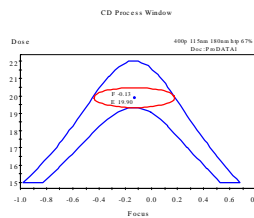
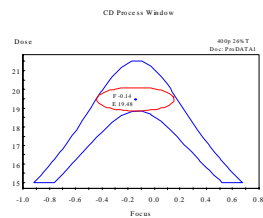
9A shows a comparison of the two masks. Clockwise from the top left is the mask layout for a 26% transmittance attenuated phase-shifting mask, the layout for an unattenuated, chromeless phase-shifting mask that has been halftoned to make its diffraction pattern similar to that of the 26% attenuated mask, the aerial image of the halftone mask, and the comparison of the diffraction orders produced by both the attenuated and the halftoned, unattenuated mask.



9B shows the focus-exposure process window for maintaining 90nm to 110nm resist linewidth sizing. Clockwise from the top left, the process window for the 26% attenuated phase-shifting mask, the process window for the halftone, unattenuated phase-shifting mask, the percent exposure latitude for both masks, an overlay of the process windows for the two masks.

26%T Attenuated PSM

100%T Halftone PSM



Focus-Exposure Resist Response Comparison

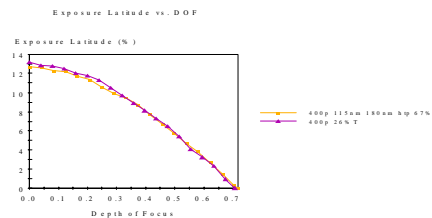
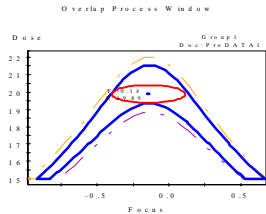


Figure 10 shows how two features that have different optimal transmissions for image quality can be half-toned so that they all have optimal imaging capability using the same attenuated phase-shifting material.

10A shows unmodified chromeless phase-shift patterns in the top row and the modified patterns in the bottom row.

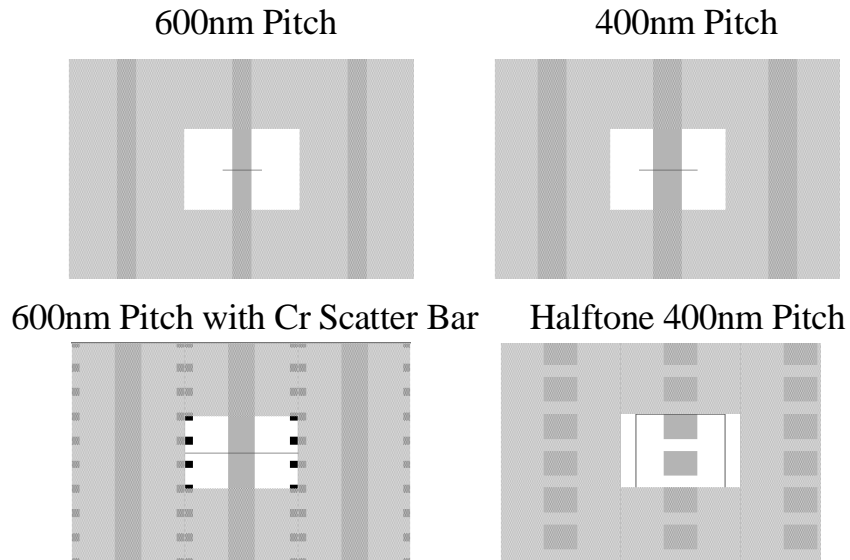
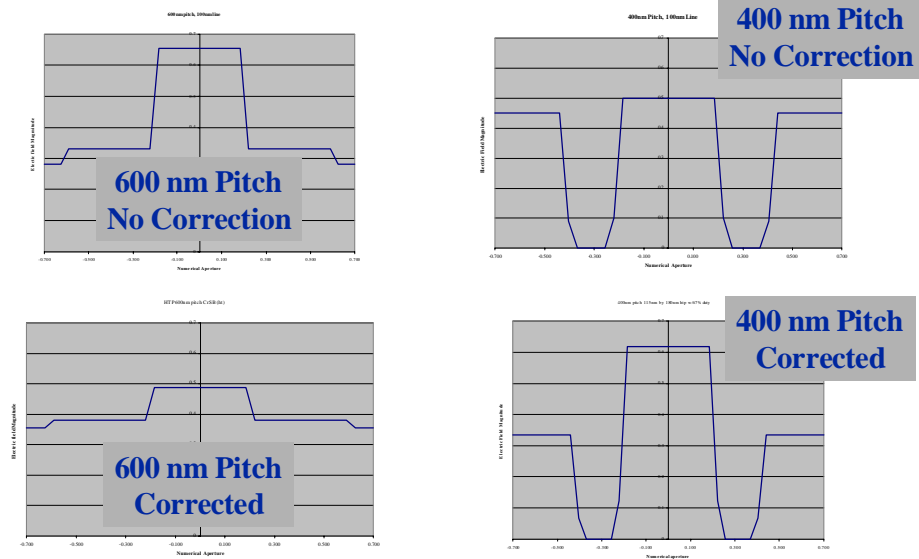
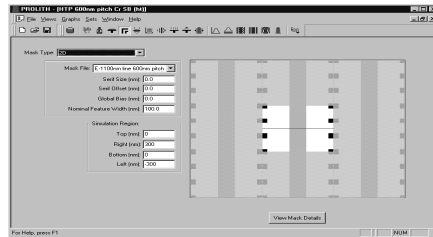


Figure 10B shows the diffraction pattern for the object pattern before and after modification.

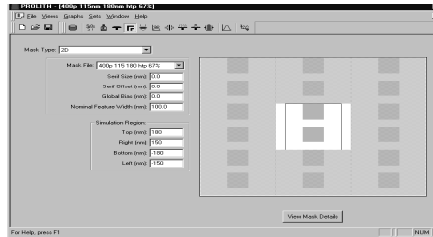


10C shows that a 600nm-400nm pitch common focus-exposure corridor is produced using the 400nm pitch pattern modifications from 9B.

600nm Pitch



400nm Pitch



Focus-Exposure Common Process Window Information

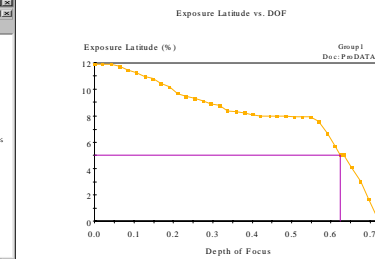
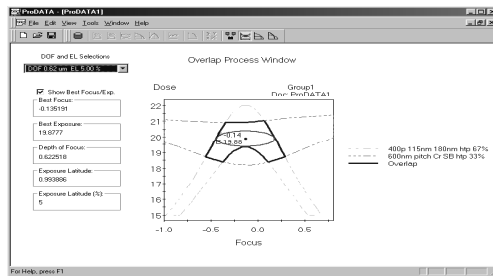
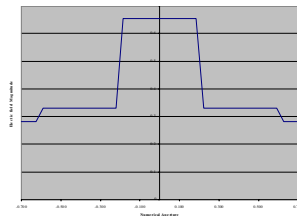
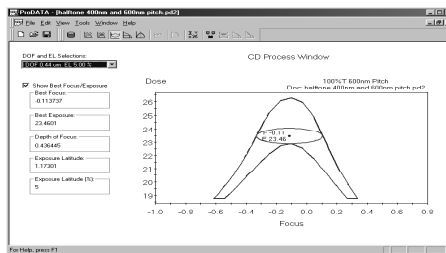
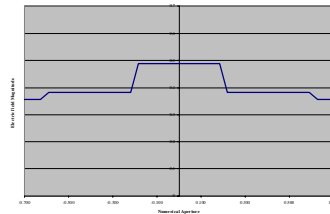


Figure 11 shows how the focus-exposure process window is enhanced using scattering bars to suppress zero diffraction order. Clockwise from the top left shows the diffraction order for an uncorrected 100nm line with a 600nm pitch, the diffraction orders for a corrected layout, the process window for the corrected layout, and the process window for the uncorrected layout. Note that the corrected mask has four times the depth of focus of the uncorrected mask.

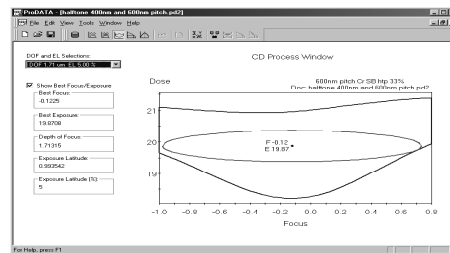
600nm Pitch without Correction



600nm Pitch with Correction



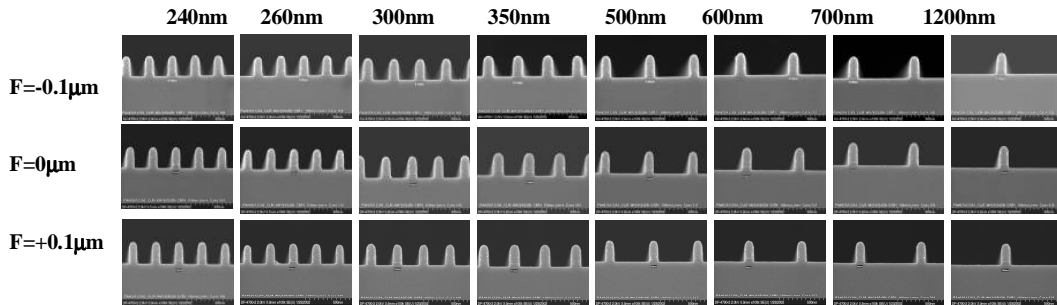
Depth of focus = 0.4 microns



Depth of focus = 1.7 microns

Figure 12 shows through focus images of resist for pitches of 240nm, 260nm, 300nm, 350nm, 500nm, 600nm, 700nm and 1200nm. Exposure was made with an ASML PAS 5500/800 0.8 NA and quasar illumination with inner sigma of 0.57 and outer of 0.87.

100nm ($k_1=0.32$) 1-D Line Spaces Exposed on ASML /800 with CPL



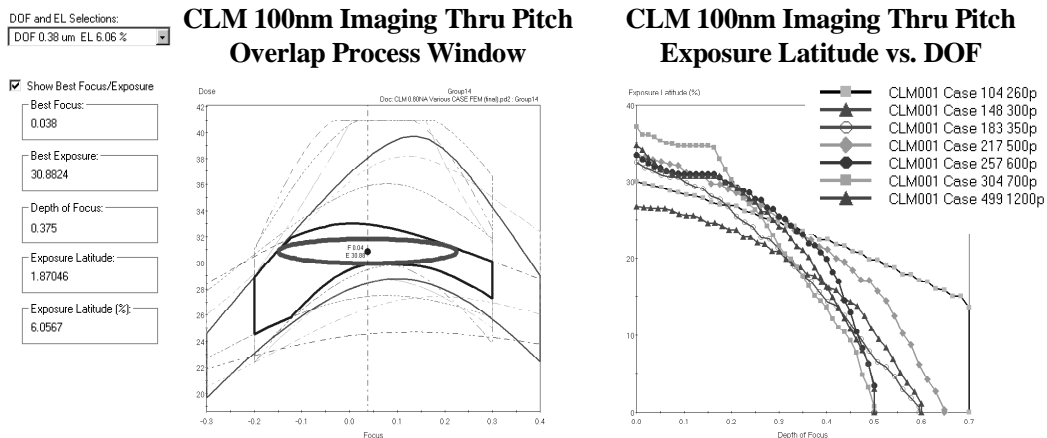
Customer Process

- 100nm imaging through pitch
- 220nm of resist
- ASML PAS 5500/800 NA=0.8 Quasar $s_{in}=0.57$ $s_{out}=0.87$

No Forbidden Pitches

Some top rounding in the resist

Figure 13 shows experimental focus-exposure resist linewidth results for pitches of 240nm, 260nm, 300nm, 350nm, 500nm, 600nm, 700nm and 1200nm. Exposure was made with an ASML PAS 5500/800 0.8 NA and Quasar illumination with inner sigma of 0.57 and outer of 0.87.



0.38µm DoF @ 6% EL

Table 1 describes the mask patterns shown in Figures 12 and 13.

Case	Pitch	LW	HP	HD	BW	BHD	BD
#	nm	nm	nm	%	nm	%	nm
118	260	100	180	67	0	NA	0
152	300	110	180	67	0	NA	0
183	350	120	180	67	0	NA	0
217	500	100	180	100	0	NA	0
257	600	100	180	100	100	33	1
304	700	90	180	100	80	33	1
438	1200	80	180	100	100	33	200

Definitions

Case = reference number from look up table

Pitch = center of primary to center of adjacent primary feature

LW = linewidth of primary feature

HP = halftone pitch of primary feature

HD = halftone duty cycle = PI_shifted-length divided by HP

BW = width of phase-shifted assist feature (no chrome assists used in this work)

BHD = halftone duty cycle of assist feature

BD = separation of primary and assist features, 1 means assist is positioned in center of space

Figure 14 shows top-down to cross-section SEM correlation and Pareto analysis.

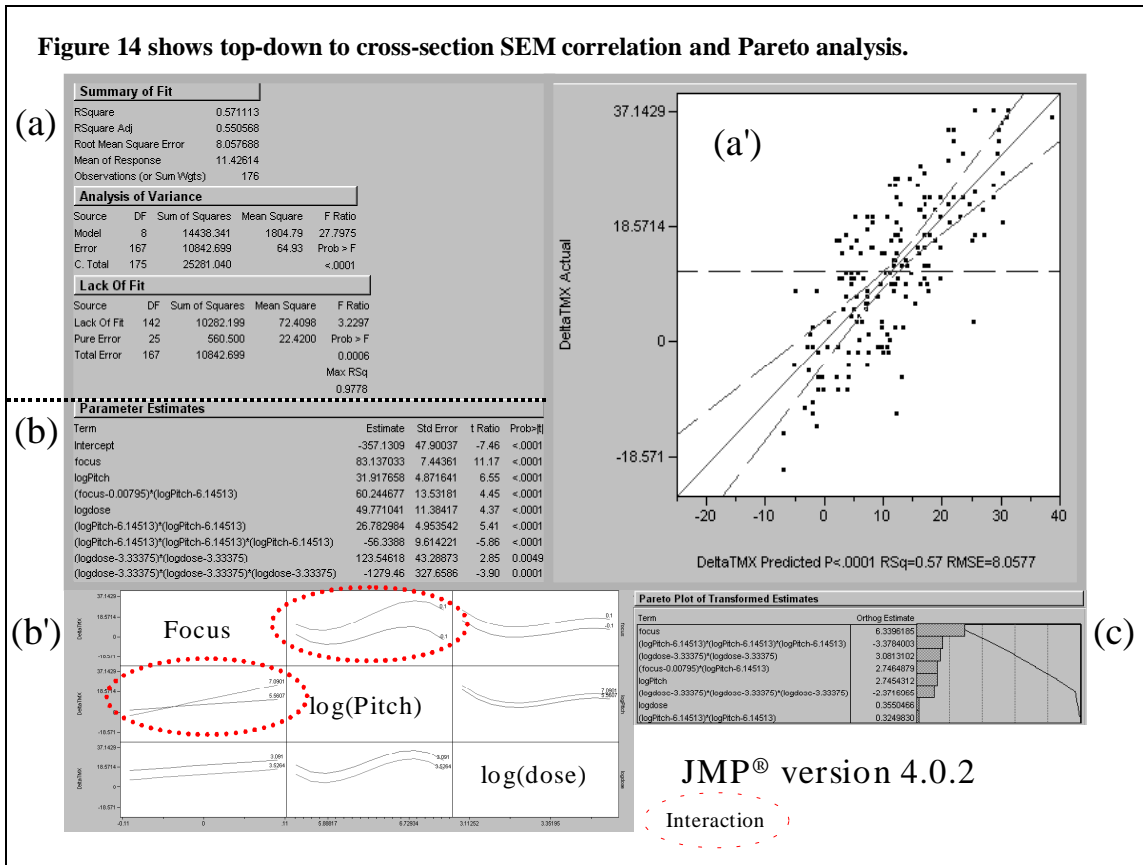
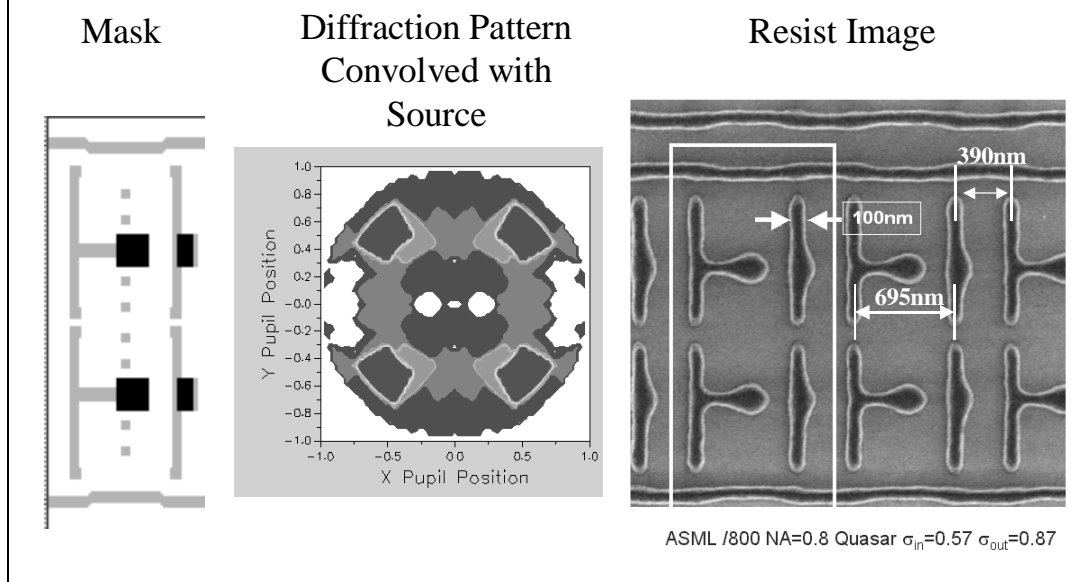


Figure 15 shows the imaging of a 6 transistor SRAM with a cell pitch of 1085nm in the x-orientation, the figures, from left to right are, hybrid mask, diffraction pattern convolved with the source and the resist image. Exposure was made with an ASML PAS 5500/800 0.8 NA and Quasar illumination with inner sigma of 0.57 and outer of 0.87.



7.0 References

- ¹ Socha et al., **SPIE 3748**, pp. 290-314 (1999).
- ² Petersen et al., **SPIE 3546**, pp. 288-303 (1998).
- ³ M. D. Levenson, **Physics Today**, pp. 28-36 (July 1993).
- ⁴ C. A. Mack, **KTI Microlithography Seminar: Interface'91**, pp. 23-35 (1991).
- ⁵ T. A. Brunner, **SPIE 1927**, pp. 54-62 (1993).
- ⁶ J. F. Chen et al, **SPIE 4346**, pp. 515-533 (2001). (Note that this paper has an excellent bibliography concerning chromeless phase shift.)
- ⁷ US Patent 6,335,130